Biochimica et Biophysica Acta 1852 (2015) 1574–1584

Contents lists available at ScienceDirect

Biochimica et Biophysica Acta

journal homepage: www.elsevier.com/locate/bbadis

TIPE2 protein prevents injury-induced restenosis in mice

Guizhong Zhang [a], Lianying Zhao [c], Yiyao Wang [a], Jie Shao [a], Jian Cui [a], Yunwei Lou [a], Minghong Geng [a], Na Zhang [a], Youhai H. Chen [b], Suxia Liu [a,*]

[a] Department of Immunology, Shandong University School of Medicine, Ji'nan, PR China
[b] Department of Pathology and Laboratory Medicine, University of PA, Philadelphia, USA
[c] Department of Anesthesiology, Qilu Hospital of Shandong University, PR China

ARTICLE INFO

Article history:
Received 1 December 2014
Received in revised form 15 April 2015
Accepted 16 April 2015
Available online 22 April 2015

Keywords:
TNFAIP8L2 (TIPE2)
Vascular smooth muscle cell
Restenosis
Rac1
STAT3

ABSTRACT

Proliferation of vascular smooth muscle cells (VSMCs) plays an important role in restenosis, a disease characterized by smooth muscle cell hyperplasia and neointimal formation. How proliferation signals are controlled to avoid restenosis is not fully understood. Here we report that TIPE2, the tumor necrosis factor (TNF) α-induced protein 8-like 2 (TNFAIP8L2), suppresses injury-induced restenosis by inhibiting VSMCs proliferation. TIPE2 was significantly upregulated in VSMCs in response to PDGF-BB stimuli and injury. Enforced TIPE2 expression significantly suppressed VSMCs proliferation and cell cycle progression, whereas TIPE2 deficiency in VSMCs promoted cell proliferation and upregulated the expression of Cyclins D1 and D3. TIPE2 likely regulated VSMC proliferation via Rac1-STAT3 and ERK1/2 signaling pathways. It blocked STAT3 activation and nuclear translocation in a Rac1-dependent manner. As a result, TIPE2-deficient VSMCs exhibited enhanced proliferation whereas TIPE2-deficient mice developed more severe restenosis in response to vascular injury. Conversely, adenovirus-mediated gene transfer of TIPE2 significantly reduced injury-induced restenosis in mice. These results indicate that TIPE2 plays a suppressive role in injury-induced restenosis and may serve as a new therapeutic target for treating the disease.

1. Introduction

Proliferation of vascular smooth muscle cells (VSMCs) plays a critical role in the development of vascular diseases such as restenosis following percutaneous coronary interventions (PCI) or angioplasty [1,2]. Although drug-eluting stents and continuing dual antiplatelet therapy can inhibit VSMC proliferation and subsequent restenosis, their clinical benefits are still limited because of the severe clinical complications, such as acute thrombocytopenia and late stent thrombosis [3–6]. Therefore, the identification of new antiproliferative molecules holds promise for new therapeutic strategies for treating restenosis following angioplasty and PCI.

TNFAIP8L2 (TIPE2), the tumor necrosis factor (TNF)-α-induced protein 8 (TNFAIP8, TIPE) like 2, is a member of the TNFAIP8 family that plays important roles in controlling inflammation and tumorgenesis by suppressing RAS signaling [7–10]. Its deficiency in 129/J mice causes fatal inflammatory diseases [8] and abnormal expression in humans is associated with many kinds of diseases, such as hepatocellular carcinoma [7,10], stroke [11], HBV infection [12] and atherosclerosis [13,14]. Our previous studies showed that TIPE2 plays atheroprotective roles by negatively regulating ox-LDL-induced inflammatory responses in macrophages [13,14]. Furthermore, TIPE2 could inhibit neointima formation by regulating phenotypic switching of VSMCs during atherogenesis [13,14]. However, whether TIPE2 plays a role in the vascular remodeling process in response to injury is still unknown. We report here that TIPE2 could suppress experimental restenosis by inhibiting vascular remodeling after injury.

2. Materials and methods

2.1. Mice

All experiments with animals were performed in accordance with the National Institutes of Health Guide for the Care and Use of Laboratory Animals (NIH publication numbers 23–80, 2011) and the Animal Management Guidelines of the Chinese Ministry of Health (document no. 55, 2001). All animal procedures were approved by the Animal Ethical Committee of the Shandong University. Male wide type (WT) C57BL/6J mice were purchased from Shanghai Laboratory Animal Center of the Chinese Academy of Science, and were 8–12-weeks-old at the time of the entry into the study. The male TIPE2-deficient (*TIPE2*$^{-/-}$) C57BL/6J mice of the same age were as described previously [8]. All mice were housed in the Animal Facilities of the Shandong University, under pathogen-free condition.

* Corresponding author at: 44# Wenhua West Road, Department of Immunology, Shandong University School of Medicine, Ji'nan 250012, PR China. Tel.: +86 531 88382038; fax: +86 531 88382084.
E-mail address: suxiasd@163.com (S. Liu).

http://dx.doi.org/10.1016/j.bbadis.2015.04.018
0925-4439/

2.2. Experimental restenosis

TIPE2$^{-/-}$ or WT mice were utilized to perform carotid artery ligation to induce restenosis as described previously [15]. Mice were anesthetized with sodium pentobarbital (50 mg/kg, i.p.). The adequacy of anesthesia was monitored by testing respiration rate, mucous membrane color and tactile stimulus response. After adequate anesthesia, the left carotid artery was completely ligated just proximal to the carotid bifurcation. The right carotid artery served as an uninjured control. Both the left and right carotid arteries were collected at 7, 14, and 21 days after injury. Before isolation of tissues, mice were deeply anesthetized with 5% isoflurane and rapidly perfused via the aorta with 37 °C warm saline followed by 4% paraformaldehyde. The carotid artery was removed and fixed in 4% paraformaldehyde overnight, then embedded in optimal cutting temperature (OCT) compound (Tissue-Tek; Sakura Finetek). Cross sections at 5 μm thickness were prepared from tissues 1.0 mm proximal to the ligature of the aortic arch. These sections were located at ~2.0 mm proximal to the ligature, and each section was 300 μm apart (i.e., 1700 μm, 2000 μm, and 2300 μm proximal to the ligature) [16]. Sections were subjected to hematoxylin (Sigma Diagnostics) and eosin (Merck Diagnostica) staining, and the areas of the intima and media were measured by Image-Pro Plus software (Media Cybernetics, Silver Spring, MD). Morphologic analysis was performed for 3 sections per artery. Six mice for each genotype were analyzed.

All mice received intraperitoneal injection of the thymidine analog 5-ethynyl-2′-deoxyuridine (EDU, Invitrogen) at 5 μg/g of body weight for 12 h prior to euthanasia. Some sections were washed in PBS and permeabilized using 0.5% Triton X-100; the incorporated EDU was conjugated to Alexa Fluor 488-azides using the Click-IT reagent kit (Molecular Probes, Invitrogen), and stained with McAb anti- SMαA (Millipore, 1:200) and rhodamine-conjugated secondary Abs (Molecular Probes, Invitrogen). After the cell nuclei were stained with 4′, 6-diamino-2-phenylindole (DAPI, Roche), the sections were visualized by fluorescent microscopy (Olympus BX51, Japan), and the percentage of EDU-positive VSMCs was analyzed by Image-Pro Plus software (Media Cybernetics, Silver Spring, MD).

Alternatively, sections were stained with TUNEL (Roche) to detect apoptotic cells. The TUNEL Index was calculated as the ratio of the number of TUNEL-positive nuclei to the total nuclei number in the section.

2.3. Recombinant adenovirus and infection

Recombinant adenovirus encoding murine TIPE2 (mTIPE2) and GFP were prepared by Sinogenomax corporation (Beijing, China). WT mice ($n = 20$) with complete ligation in the left carotid artery were in situ infected with mTIPE2-expressed adenovirus or GFP-expressed adenovirus (1×10^9 pfu). Mice were subjected to a second infection by tail vein injection at day 21 and sacrificed at day 42. Cross-section preparation and morphologic analysis were performed as described above.

2.4. Cell culture of VSMCs

Primary murine VSMCs used in this study were obtained from the aorta ventralis of 8-week-old male WT or *TIPE2*$^{-/-}$ mice (deeply anesthetized with 5% isoflurane) by enzymatic digestion (type I collagenase and type III elastase, Sigma) according to a previous study [14]. Quiescent cells cultured in serum-free DMEM for 48 h were collected and stained with anti-SMαA; flow cytometric analysis was performed to determine the percentage of positive cells. VSMCs (SMαA-positive Cells) from passages 3 to 7 were used in this study.

2.5. Plasmids and transfection

pEGFP-mTIPE2, pRK5-flag-mTIPE2-WT and pRK5-flag-mTIPE2-R24A were constructed in our lab as described previously [9]. pRK5-myc-Rac1-Q61L and pMXs-STAT3-C were purchased from Addgene. Murine STAT3-C cDNA was subcloned from pMXs-STAT3-C. The primers used for PCR were STAT3F-BamH1 (cgcggatccgccaccATGGCT CAGTGGAACCAGCTG) and STAT3R-EcoR1 (ccggaattcTCACATGGGGG AGGTAGCACA) [17]. The PCR product was digested with BamH1 and EcoR1, cloned into pCMV-N-HA vector, and further confirmed by sequencing (Invitrogen).

Transfection was performed using Lipofectamine 2000 (Invitrogen) according to the manufacturer's protocol. WT VSMCs transfected with Flag-mTIPE2 or Flag-mTIPE2-R24A were used for determining signal pathway activation, D type Cyclin expression or cell proliferation. HEK293 cells transfected with HA-STAT3-C along with Flag-mTIPE2, Rac1-siRNA, or Flag-mTIPE2 plus Myc-Rac1-Q61L were used for STAT3-C nucleus translocation analysis.

2.6. Quantitative real-time PCR

Total RNA was extracted with TRIZOL reagent (Invitrogen) according to the protocol. Single-strand cDNA was synthesized using hexamer primers (Promega). cDNA was used as templates for the amplification of genes concerned. Specific primers used for Quantitative real-time PCR assays were 5′-GCGTACCCTGACACCAATCTC-3′ (Sense) and 5′-CTCCTCTTCGCACTTCTGCTC-3′ (Antisense) for Cyclin D1, 5′-TGGATCGC TACCTGTCCTG-3′ (Sense) and 5′-CCTGGTCCGTATAGATGCAAAG-3′ (Antisense) for Cyclin D3, 5′-TCAGAAACATCCAAGGCCAGAC-3′ (Sense) and 5′-CGGACCGACCAGCCATTTTAC-3′ (Antisense) for mTIPE2, 5′-TGCGTGACATCAAAGAGAAG-3′ (Sense) and 5′-TCCATACCCAAGAA GGAAGG-3′ (Antisense) for β-actin. Each sample was run in triplicate. The primers used throughout this study were synthesized by Invitrogen Corporation.

2.7. Proliferation

VSMCs (2×10^3 cells/well) were cultured in 96-well dishes overnight and then allowed to proliferate in the absence or presence of 10 ng/mL PDGF-BB (Pepro Tech) in DMEM (GIBCO-BRL) medium containing 10% FBS (Gibco-BRL). Cell proliferation was measured at different time intervals over a period of 3 days using Cell Counting Kit-8 reagent (CCK-8, Dojindo) as described by the manufacturer. At each time point, 10 μL of CCK-8 reagent was added to each well 1 h before the end of incubation. The optical density (OD) value of each sample was measured at a wavelength of 450 nm on a microplate reader (Model 680, BIO-RAD).

2.8. Flow cytometry analysis

VSMCs were cultured in 6-well dishes for 24 h. Then cells were made quiescent by incubation with serum-free DMEM for 24 h, and allowed to grow for another 24 h in the absence or presence of PDGF-BB (10 ng/mL). Cells were collected, fixed in ice-cold ethanol, and treated with 100 μg/mL RNase A solution in 37 °C for 30 min. Cells were then washed and incubated with 50 μg/mL propidium iodide (PI, Sigma) containing 0.2% Triton X-100 for 30 min. PI incorporation was determined by flow cytometry (FC-500 MCL/MPL, BECKMAN).

2.9. Western blot and antibodies

Western blotting was performed as described previously [14]. The following primary antibodies were used: anti-SMαA (Millipore, 1:1000), anti-Rac1 and GTP-Rac1 (Santa Cruz and NewEast Bioscience respectively, 1:500); anti-ERK and p-ERK, anti-STAT3 and p-705Tyr-STAT3 (Cell Signaling Technology, 1:1000); anti-Cyclin D1 and anti-Cyclin D3 (Bioworlde, 1:500); anti-β-actin (ZSGB-BIO, 1:1000), anti-flag, anti-myc, anti-HA (Sigma, 1:1000); anti-β-Tubulin and anti-lamin A/C (Bioworlde, 1:1000). TIPE2 was detected using a specific antibody as described previously [18]. Immunoblotting

was conducted by incubating the membranes with primary antibodies at 4 °C overnight followed by secondary antibodies (goat anti-rabbit Ig G or goat anti-mouse Ig G, 1:1000) conjugated with peroxidase for 1 h at room temperature. After washing, bound peroxidase activity was detected by the ECL detection system (ECL, F-cheiBIsi.6pro, DNR) using the SuperSignal West Pico kit (Pierce Biotechnology). Densitometric analysis was performed using Image-Pro Plus software (Media Cybernetics, Silver Spring, MD).

2.10. PBD pull-down assay

VSMCs (2×10^5 cells/well) were cultured in 6-well dishes for 24 h. Then cells were made quiescent by incubation with serum-free DMEM for 24 h, and stimulated with PDGF-BB (10 ng/mL) for 15 or 30 min. Then cells were washed in PBS and lysed in PBD lysis buffer (50 mM Tris, pH 7.5, 10 mM $MgCl_2$, 0.2 M NaCl, 0.5% Nonidet P-40, and 1× protease inhibitors mixture) (Roche). The lysate was incubated with 20 μg of p21-activated kinase (PAK)-GST protein beads (Cytoskeleton) for 30 min at 4 °C. After washing, protein on beads and in total cell lysates was subjected to Western blot to determine the level of active Rac1.

2.11. Immunofluorescence and microscopy

Quiescent WT or *TIPE2*$^{-/-}$ VSMCs, HEK293 transfected with pEGFP-mTIPE2/HA-STAT3-C or pEGFP/HA-STAT3-C, HEK293 transfected with Rac1-siRNA/HA-STAT3-C or MOCK/HA-STAT3-C were treated with 10 ng/mL of PDGF-BB for 15 min and then were washed, fixed in 4% paraformaldehyde, and permeabilized with 0.5% Triton X-100. Cells were blocked with goat serum and incubated with the first antibody followed by goat anti-rabbit antibody. Rabbit anti-STAT3 (Cell Signaling Technology, 1:100) and rabbit anti-HA (Sigma, 1:500) antibodies (Abs) were used as the first Abs. Alexa 488- or rhodamine-conjugated goat anti-rabbit immunoglobulin (Molecular Probes) was used as the secondary Ab. DNA staining was performed using 4, 6-diamino-2-phenylindole (DAPI, Roche).

Fixed fluorescent images were analyzed on an optical microscope (Olympus BX51, Japan). 10–15 high-power fields were evaluated, and representative images were shown. Experiments were repeated three times, and each treatment was done in duplicate.

2.12. Subcellular fractionation

Cytoplasmic and nuclear proteins were isolated with NE-PER (R) Nuclear and Cytoplasmic Extraction Reagents (Pierce Biotechnology). In brief, cells were washed with cold PBS and fully suspended in ice-cold CER I by vortex on the highest setting for 15 s, followed by incubation on ice for 10 min. Homogenates were mixed with ice-cold CER II, incubated on ice for 1 min and then centrifuged at 16,000 ×*g* for 5 min at 4 °C. The supernatants (cytosol) were collected and the pellets were re-suspended in ice-cold NER and incubated on ice for 40 min, vortexed for 15 s every 10 min. The lysates were again centrifuged at 16,000 ×*g* for 5 min, and the supernatants (nucleus) were collected. The distributions of proteins in the cytosol and nucleus fractions were analyzed by Western blot.

2.13. Statistical analysis

All analyses were performed using SPSS 16.0 (SPSS Inc.). Data were expressed as mean ± SEM. Student's *t*-test was used to compare continuous data for two groups, ANOVA was used for comparisons among multiple groups, and LSD post-hoc test was used for multiple comparisons. $P < 0.05$ was considered statistically significant. All experiments were repeated at least three times.

3. Results

3.1. TIPE2 suppresses injury-induced restenosis in mice

To evaluate the role of TIPE2 in restenosis, ligation-induced vascular injury was generated in the left carotid artery of WT and *TIPE2*$^{-/-}$ mice. As shown in Fig. 1A, significantly enhanced neointimal formation was observed in *TIPE2*$^{-/-}$ mice at days 14 and 21 after vascular injury compared with WT mice. Furthermore, in injury-induced restenosis groups, neointimal area was significantly larger in *TIPE2*$^{-/-}$ mice than WT controls, 1.9-fold larger at day 14, and 3.7-fold larger at day 21 after injury (Fig. 1B left panel). Consistent with these results, an increased I/M (Intimal/Media) ratio in *TIPE2*$^{-/-}$ mice was observed at day 14 (*TIPE2*$^{-/-}$ vs. WT, 0.739 ± 0.1075 (n = 5) vs. 0.416 ± 0.0601 (n = 5), $P = 0.0252$) and day 21 (*TIPE2*$^{-/-}$ vs. WT, 2.422 ± 0.2101 (n = 5) vs. 0.517 ± 0.0812 (n = 5), $P < 0.0001$) after injury (Fig. 1B, right panel). These results suggest that TIPE2 deficiency accelerates the restenosis response to vascular injury.

To confirm the inhibitory effects of TIPE2 on restenosis, therapeutic experiments were performed with recombinant adenovirus-mediated overexpression of mTIPE2 in injured vasculature of WT mice. The results showed that TIPE2 significantly delayed injury-induced neointimal formation (Fig. 1C, D). Six weeks after injury, both of neointimal area and I/M ratio were remarkably reduced by TIPE2-expressing adenovirus (Fig. 1D, Ad-GFP vs. Ad-mTIPE2, 37.78 ± 2.402 × 10^3 μm^2 (n = 8) vs. 19.36 ± 2.905 × 10^3 μm^2 (n = 12), $P = 0.0081$ for neointimal area; 1.885 ± 0.1794 (n = 8) vs. 0.8888 ± 0.1374 (n = 12), $P = 0.0116$ for I/M ratio). These data further demonstrated that TIPE2 could lessen restenosis after injury.

Recent studies showed that wire injury-induced neointimal hyperplasia could primarily be attributed to the proliferation of VSMCs [6,19]. Our previous study showed that TIPE2 played atheroprotective roles by regulating phenotypic switching of VSMCs [14]. Therefore, we examined the cellular proliferation in carotid arteries by EDU staining. Intriguing, EDU-positive cells in arteries were significantly increased in *TIPE2*$^{-/-}$ mice (Fig. 1E, left panel). At day 7 after injury, a higher percentage of EDU-positive cells was observed in *TIPE2*$^{-/-}$ mice than WT mice controls (Fig. 1E, right panel, *TIPE2*$^{-/-}$ vs. WT, 21.69 ± 2.639% (n = 5) vs. 9.58 ± 1.625% (n = 5), $P = 0.0175$). These data suggest that TIPE2 might play suppressive roles on restenosis via inhibiting VSMC proliferation.

Furthermore, TIPE2 can promote tumor cell death [10]. We don't know whether the enhanced neointima formation in *TIPE2*$^{-/-}$ mice is associated with VSMC apoptosis. To address this issue, we detected the apoptotic cells in the arteries through TUNEL assay. As shown in Fig. 1F, both *TIPE2*$^{-/-}$ mice and WT mice exhibited low levels of apoptosis, and there was no significant difference between these two groups (*TIPE2*$^{-/-}$ vs. WT, 2.37 ± 0.841% (n = 4) vs. 2.57 ± 0.673% (n = 3), $P = 0.8565$). These data suggest that constitutive TIPE2 inhibited VSMC proliferation without affecting apoptosis in the pathologic condition of experimental restenosis.

3.2. TIPE2 is markedly upregulated in VSMC response to PDGF-BB stimulation and injury

To study the mechanism of TIPE2 in VSMC proliferation, primary VSMCs were isolated from WT and *TIPE2*$^{-/-}$ mice and identified using an antibody directed against SMαA protein by flow cytometry analysis. We found that more than 95% of isolated cells (WT and *TIPE2*$^{-/-}$ VSMCs) were SMαA-positive (Fig. 2A).

Platelet-derived growth factor (PDGF) plays a central role in the pathogenesis of intimal hyperplasia and mediates VSMC proliferation [1]. To evaluate the effect of PDGF on TIPE2 expression, WT VSMCs were grown in DMEM medium containing 10% FBS in the absence or presence of 10 ng/mL PDGF-BB. As shown in Fig. 2B and C, both the mRNA and protein levels of TIPE2 in WT but not *TIPE2*$^{-/-}$ VSMCs

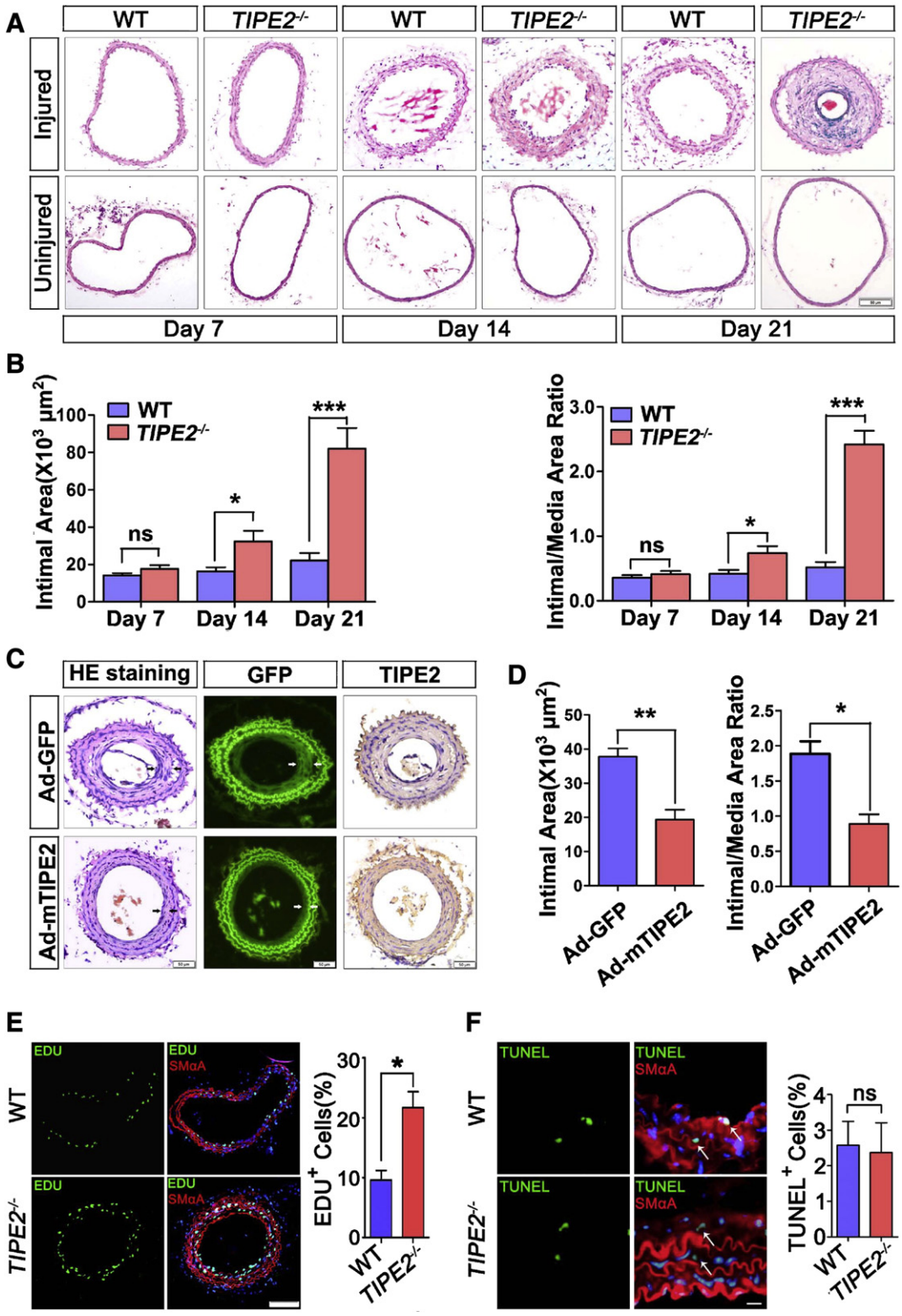

Fig. 1. TIPE2 suppresses injury-induced neointimal formation in mice. (A) Representative microphotographs of hematoxylin eosin (HE)-stained uninjured or injured carotid arterial in WT and *TIPE2*$^{-/-}$ mice at days 7, 14, and 21 after injury. Scale bar indicates 50 μm. (B) Quantitative analysis of intimal area (n = 5) and I/M ratio (n = 5) as shown in (A). (C) Representative microphotographs of HE-stained neointimal sections obtained from carotid-injured WT mice at day 42 after adenovirus-mediated gene transfer of murine TIPE2 (mTIPE2). Scale bars indicate 50 μm. (D) Quantitative analysis of the intimal area (Ad-GFP, n = 8; Ad-mTIPE2, n = 12) as shown in (C). (E) Representative magnifications (left panel) and quantitative analysis (right panel, n = 5) of the EDU incorporation in VSMCs of carotids at day 7 after injury. Scale bars indicate 50 μm. (F) Representative magnifications (left panel) and quantitative analysis (right panel, n = 3 for WT, n = 4 for *TIPE2*$^{-/-}$ mice) of the TUNEL staining in VSMCs of carotids at day 14 after injury. Scale bars indicate 20 μm.

were increased significantly following PDGF-BB stimulation. Consistent with this finding, TIPE2 was upregulated in response to injury in vascular media of WT mice (Fig. 2D). However, the increased tendency of TIPE2 was lessened at day 14 compared with day 7 after injury (Fig. 2D), providing a plausible explanation that WT mice couldn't completely avoid injury-induced restenosis (Fig. 1C, D, Ad-GFP

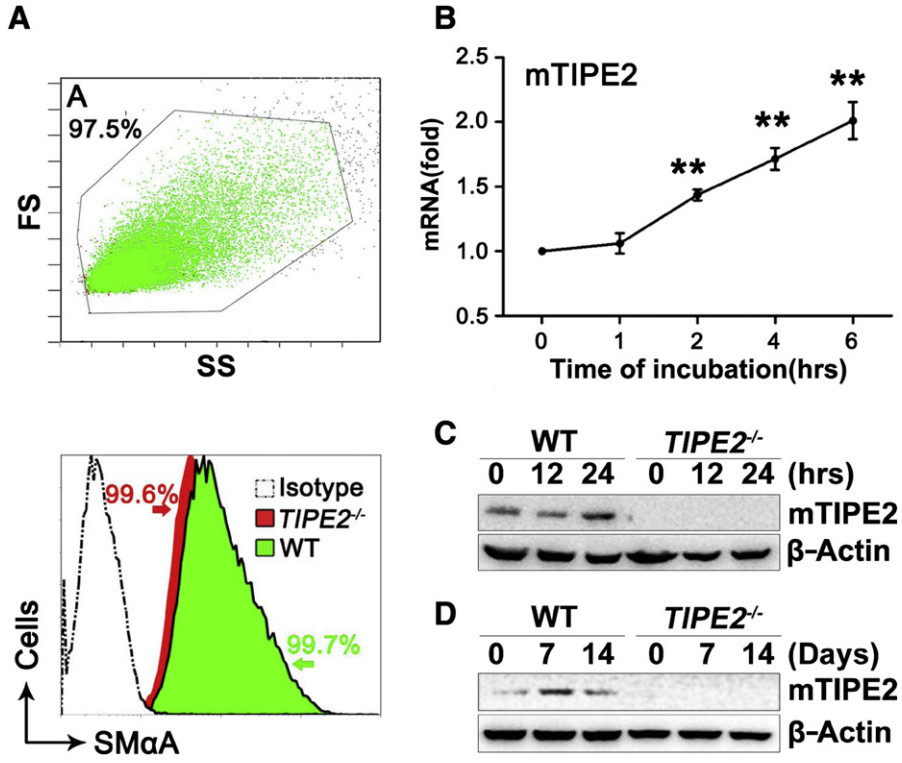

Fig. 2. TIPE2 is upregulated in VSMCs in response to PDGF-BB or injury. (A) Flow cytometric analysis of cultured VSMCs. (B) TIPE2 mRNA levels in VSMCs treated with PDGF-BB (10 ng/mL) for the indicated time points were measured by real-time PCR. $^{**}P < 0.005$, n = 3. (C) Levels of TIPE2 protein in WT and *TIPE2*$^{-/-}$ VSMCs treated with PDGF-BB (10 ng/mL) were detected by immunoblotting; β-actin served as a loading control. One representative result of three independent experiments was demonstrated. (D) Expression of TIPE2 protein in injured carotids obtained from WT (n = 5) and *TIPE2*$^{-/-}$ (n = 5) mice at days 7 and 14 post vascular injury was determined by immunoblotting; β-actin served as a loading control.

group). Taken together, these results indicate that TIPE2 may affect restenosis by regulating VSMC functions.

3.3. TIPE2 deficiency promotes VSMC proliferation by upregulating Cyclin D1 and D3 expression

To investigate the functional role of TIPE2 on VSMC proliferation, we examined the effect of TIPE2 deficiency on these PDGF-BB-induced cellular processes. As shown in Fig. 3A, TIPE2 deficiency significantly enhanced VSMC proliferation either in the presence or absence of PDGF-BB stimuli. Fluorescence-activated cell-sorting analysis of PI-stained cells also indicated a cell cycle arrest in the G_0/G_1 phase caused by TIPE2 (Fig. 3B). As shown in Fig. 3C, TIPE2 deficiency increased the proportion of VSMC in S phase (untreated: *TIPE2*$^{-/-}$ vs. WT, 12.17 ± 0.436% (n = 5) vs. 6.00 ± 0.351% (n = 5), $P = 0.0004$; PDGF-BB-treated: 41.61 ± 2.138% (n = 5) vs. 19.12 ± 0.944% (n = 5), $P = 0.0007$), and simultaneously reduced the percentage of cells in the G_0/G_1 phase (untreated: *TIPE2*$^{-/-}$ vs. WT, 82.68 ± 1.168% (n = 5) vs. 90.29 ± 1.536% (n = 5), $P = 0.0169$; PDGF-BB-treated: 50.69 ± 1.112% (n = 5) vs. 76.11 ± 1.894% (n = 5), $P = 0.0003$). In accordance with these findings, TIPE2 ablation increased expression of Cyclins D1 and D3, which are essential for the G_1/S phase transition, in PDGF-BB-treated VSMCs (Fig. 3D, E) and injured vascular media in mice (Fig. 3F). The dedifferentiation state characterized by downregulation of differentiated marker genes, such as SMαA, SM22α, and SMMHC, is necessary for VSMC proliferation. Therefore, we determined the expression level of SMαA, and found a marked decrease in untreated or PDGF-BB-treated VSMCs and injured vascular media obtained from TIPE2-deficient mice (Fig. 3D, E). These data suggest that TIPE2 may inhibit VSMC proliferation by dampening Cyclin D1 and D3 expression.

3.4. TIPE2 significantly suppresses VSMC proliferation through sequestering cells in the G_0/G_1 phase

As determined by cell counting kit-8 analysis, TIPE2 overexpression remarkably restrained the viability of VSMCs both under resting and PDGF-BB-stimulated conditions compared with pRK5 control or R24A mutant group (Fig. 4A). Fluorescence-activated cell-sorting analysis showed that TIPE2 sequestered VSMCs in the G_0/G_1 phase (Fig. 4B and C), while R24A, a TIPE2 mutant that is not able to bind to Rac1 [9], failed to do so. This result is consistent with the effect of TIPE2 on Cyclins. As shown in Fig. 4D and E, both at the levels of transcription and translation, TIPE2 but not R24A overexpression significantly inhibited Cyclin D1 and D3 expression in VSMCs treated with or without PDGF-BB. TIPE2 overexpression significantly increased SMαA expression. As a result the dedifferentiation of TIPE2-overexpressed VSMCs in response to PDGF-BB stimulation was repressed. However, R24A had no effect on these processes (Fig. 4E). These data indicate that TIPE2 could inhibit VSMC survival by arresting cells in the G_0/G_1 phase in a Rac1-dependent manner.

3.5. TIPE2 regulates VSMC proliferation via Rac-STAT3 and Rac-ERK1/2 signaling pathways

Rac signaling is involved in the control of cell–cell adhesions, cell-matrix adhesions, cell migration, cell cycle progression, and cellular transformation [20]. Previous reports pointed out that TIPE2 inhibited Rac membrane translocation, Rac activation and downstream signaling [9]. Therefore, we examined the effect of TIPE2 on Rac1 activation in VSMCs. As shown in Fig. 5A, TIPE2 deficiency in VSMCs markedly enhanced Rac1 activation in response to PDGF-BB stimulation. Whereas overexpression of TIPE2 significantly inhibited Rac1 activation (Fig. 5B).

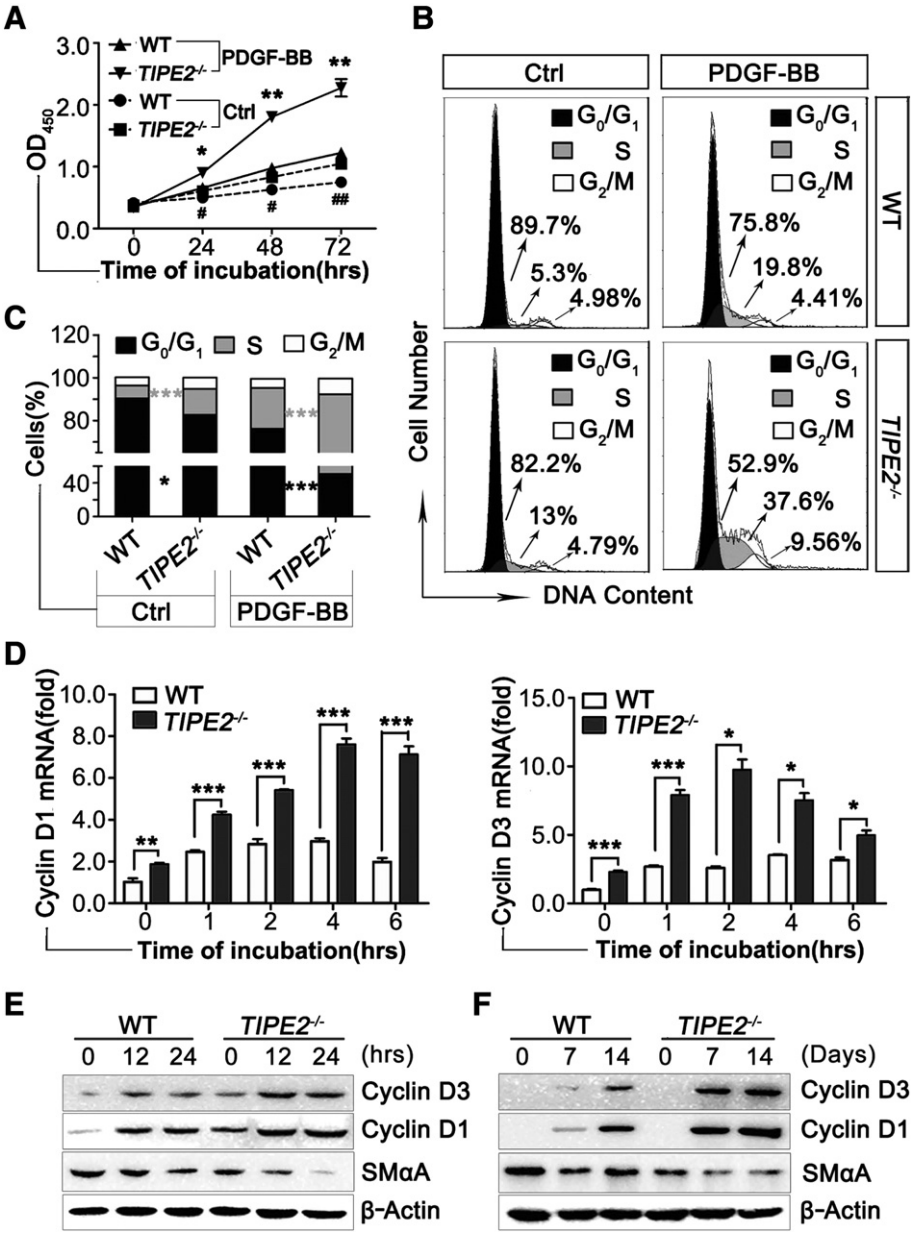

Fig. 3. TIPE2 deficiency enhanced PDGF-BB- and injury-induced Cyclin D expression and subsequent VSMC proliferation. (A) Proliferation ability of WT and *TIPE2*$^{-/-}$ VSMCs cultured in the absence or presence of PDGF-BB was examined using cell counting kit-8. $^{*}P < 0.05$, $^{**}P < 0.005$, for PDGF-BB-stimulated WT *vs* *TIPE2*$^{-/-}$ VSMCs (n = 5); $^{\#}P < 0.005$, $^{\#\#}P < 0.005$, for non-stimulated WT *vs* *TIPE2*$^{-/-}$ VSMCs (n = 5). (B) Representative graphs of cell cycle distribution determined by flow cytometric evaluation. (C) Quantification of VSMCs in G_0/G_1, S, or G_2/M phase, as determined by flow cytometric evaluation. $^{*}P < 0.05$, $^{***}P < 0.001$, n = 5. (D) Expression of Cyclin D1 and D3 mRNA in WT and *TIPE2*$^{-/-}$ VSMCs stimulated with PDGF-BB for different times was examined by real-time PCR. $^{*}P < 0.05$, $^{**}P < 0.005$, $^{***}P < 0.001$, n = 3. (E) Levels of Cyclins D1 and D3 and SMαA proteins in PDGF-BB-treated WT and *TIPE2*$^{-/-}$ VSMCs were examined by immunoblotting. One representative result of three independent experiments was shown. (F) Expression of Cyclins D1 and D3 and SMαA proteins in injured carotids obtained from WT (n = 5) and *TIPE2*$^{-/-}$ (n = 5) mice at days 7 and 14 after injury was examined by immunoblotting.

Not surprisingly, R24A was unable to suppress Rac1 activation (Fig. 5B). We also found that the phosphorylation levels of STAT3 (at Try705) and ERK1/2 were strikingly enhanced in TIPE2-deficient VSMCs (Fig. 5A), but were markedly decreased by TIPE2 overexpression (Fig. 5B). Furthermore, the enhanced activation of ERK1/2 and STAT3 in TIPE2-deficient VSMCs could be eliminated by NSC23766, a specific inhibitor that blocks Rac1 activation (Fig. 5C). Interestingly, as shown in Fig. 5D, the mRNA levels of Cyclins D1 and D3 were significantly decreased by PD98059 and Stattic (specific inhibitors for ERK1/2 and STAT3, respectively). Furthermore, the difference of expression levels between WT and *TIPE2*$^{-/-}$ VSMCs was also eliminated. These data strongly suggest that TIPE2 modulates VSMC proliferation through Rac1-STAT3 or/and ERK1/2 signaling pathways.

3.6. TIPE2 blocks STAT3 nuclear translocation in a Rac1 dependent manner

Activated STAT3 form homo- or hetero-dimers, and enter the nucleus, where they regulate expression of their target genes [21,22]. To determine the effect of TIPE2 on nuclear translocation of activated STAT3, subcellular distribution of STAT3 in WT and *TIPE2*$^{-/-}$ VSMCs was tested by immunofluorescence and immunoblotting. As shown in Fig. 6A and B, the levels of intranuclear STAT3 were significantly increased in *TIPE2*$^{-/-}$ VSMCs compared with WT cells treated with or without PDGF-BB. Importantly, the accumulation of STAT3 in nucleus was accompanied by the decrease in cytoplasm (Fig. 6B), strongly indicating that TIPE2 does not affect the expression of STAT3 but blocks the process of nuclear translocation.

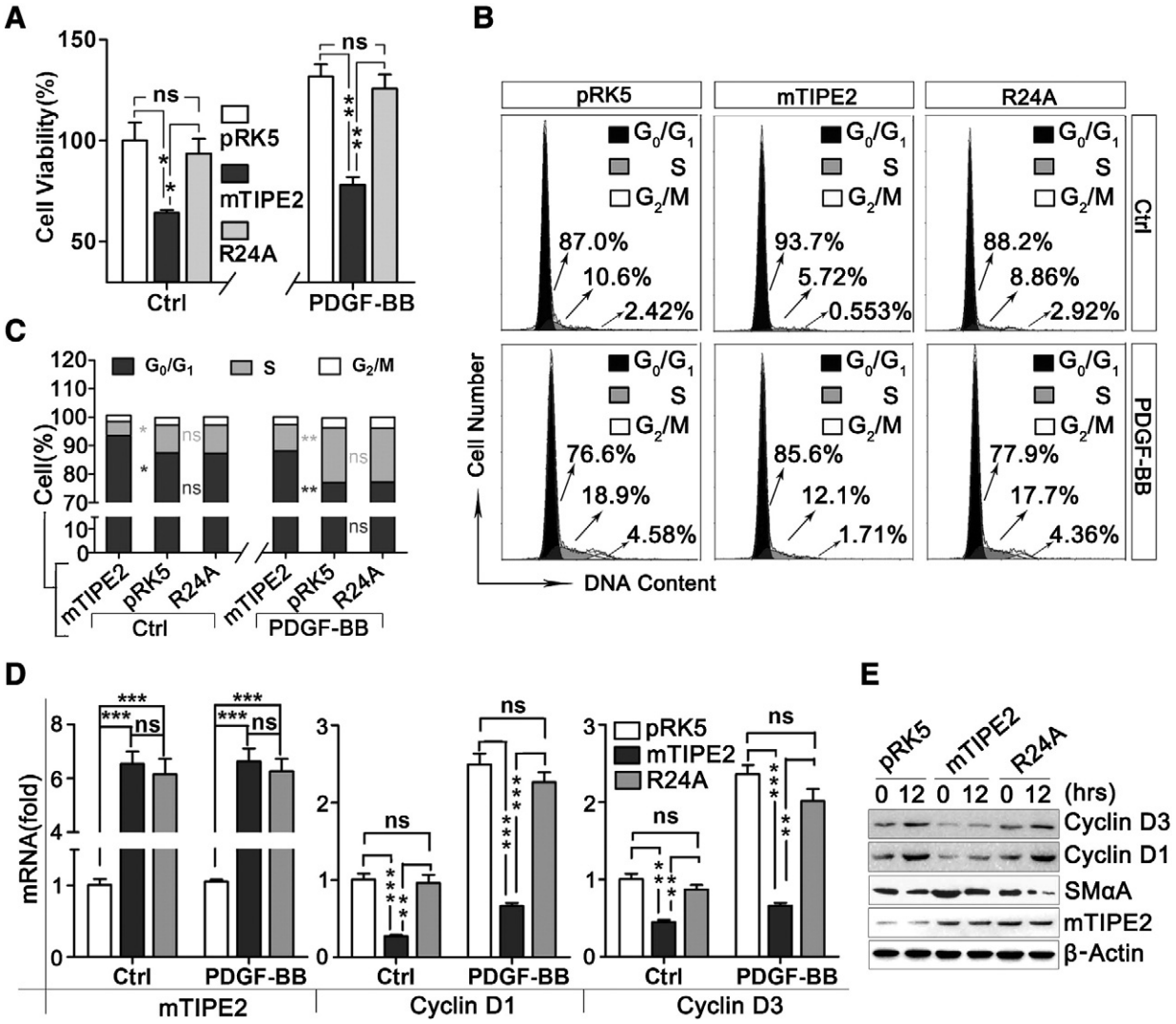

Fig. 4. TIPE2 suppresses D-type Cyclin expression and VSMCs proliferation. (A) The viability of VSMCs expressing mTIPE2 or R24A was examined using cell counting kit-8. $^{*}P < 0.05$, $^{**}P < 0.005$, n = 3. (B and C) Analysis of cell cycle of mTIPE2- or R24A-transfected VSMCs by flow cytometry. Cells transfected with pRK5 vectors were used as a control. n = 5. (D) The mRNA levels of Cyclins D1 and D3 in VSMCs expressing mTIPE2 or R24A were analyzed by real-time PCR. (F) The protein levels of Cyclins D1 and D3 and SMαA in VSMCs expressing mTIPE2 or R24A were analyzed by Western blot.

To address this issue thoroughly, STAT3-C, a dominant-active mutant of STAT3 characterized by dimerizing and entering nucleus spontaneously [23,24], was introduced into HEK293 cells. The spontaneous nuclear translocation of STAT3-C could be blocked by Rac1-siRNA (Fig. 6C, D). Therefore, we co-introduced STAT3-C and pRK5-mTIPE2 in HEK293 cells and found that overexpression of TIPE2 could significantly suppress nucleus translocation of STAT3-C (Fig. 6E). Furthermore, distribution of STAT3-C analyzed by immunoblotting revealed that both TIPE2 and Rac1-siRNA diminished accumulation of STAT3-C in the nucleus, and this inhibitory effect of TIPE2 could almost completely be abolished by Rac1-Q61L, a constitutively active form of Rac1 (Fig. 6F, left panel). This inhibitory effect and underlying mechanism of TIPE2 on STAT3-C nuclear translocation observed in HEK293 was further confirmed in WT VSMCs (Fig. 6F, right panel). Taken together, in addition to inhibiting STAT3 activation, TIPE2 also plays a negative role in nucleus translocation of STAT3.

4. Discussion

Excessive proliferation of VSMCs in the arterial wall plays a prominent role in the pathogenesis of vascular disorders such as atherosclerosis, postangioplasty restenosis, bypass vein graft failure, and cardiac allograft vasculopathy [25,26]. Elucidation of the key mechanisms controlling VSMC proliferation will help understand cellular responses to vascular injury and develop safe and efficient therapeutic strategies for the prevention of vascular proliferative diseases.

In this study we demonstrate that TIPE2, a negative regulator of inflammation and oncogenesis, prevents the development of experimental restenosis by inhibiting VSMC proliferation. We provide evidence that TIPE2 also inhibits Rac1 activation in VSMCs and interferes with downstream signaling to STAT3 and ERK1/2 in response to injury or mitogenic stimuli. Both STAT3 and ERK1/2 signal pathways are reported to be essential for the induction of cell cycle entry [26–29]. In concert with the regulation of STAT3 and ERK1/2, TIPE2 prevents the transcriptional activation of G1 phase Cyclins and subsequent G1/S phase transition, resulting in growth inhibition of VSMCs (Fig. 7).

The key findings of the present study are as follows: (1) Restenosis formation was enhanced in *TIPE2*$^{-/-}$ mice after vascular injury, which was related to an increased ratio of EDU-positive VSMCs in vivo. (2) TIPE2 expression was upregulated in response to injury and PDGF-BB stimulation in VSMCs, but it failed to completely inhibit VSMC proliferation and neointimal formation. (3) Adenovirus-mediated gene transfer of TIPE2 in vivo significantly delayed neointial formation. (4) TIPE2 prevented PDGF-BB-induced upregulation of Cyclins D1 and D3, and

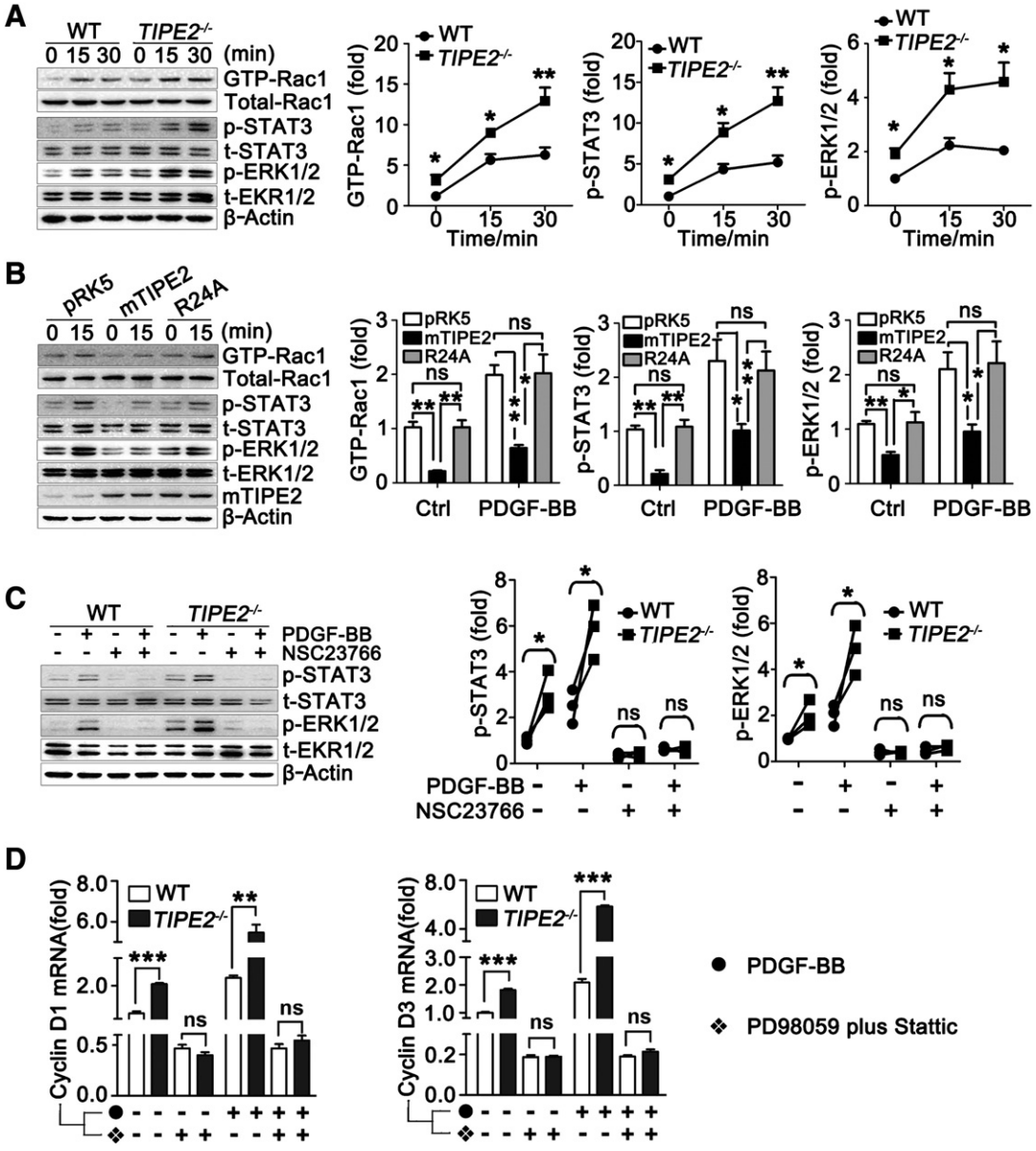

Fig. 5. TIPE2 regulates Cyclin D1 and D3 expression in a Rac-STAT3 and Rac-ERK1/2 dependent manner. (A) PDGF-BB-induced activation of Rac1, STAT3, and ERK1/2 in WT and *TIPE2*$^{-/-}$ VSMCs were examined by immunoblotting. One representative result of three independent experiments was shown (left panel). The results of quantitative analysis for the activation of Rac1, STAT3 and ERK1/2 were shown (right panel, n = 3 per group). $^{*}P < 0.05$, $^{**}P < 0.005$, ns indicated no significant difference. (B) Representative immunoblotting images for GTP-Rac1, p-STAT3, and p-ERK1/2 in mTIPE2- and R24A-transfected VSMCs (left panel). The results of quantitative analysis for the activation of Rac1, STAT3 and ERK1/2 were shown (right panel, n = 3 per group). $^{*}P < 0.05$, $^{**}P < 0.005$, ns indicated no significant difference. (C) Activation of STAT3 and ERK1/2 in WT and *TIPE2*$^{-/-}$ VSMCs incubated with NSC23766 (a specific inhibitor for Rac1, 50 μM) following PDGF-BB stimuli was determined by immunoblotting (left panel). The results of quantitative analysis for the activation of Rac1, STAT3 and ERK1/2 were shown (right panel, n = 3 per group). $^{*}P < 0.05$, ns indicated no significant difference. (D) The mRNA levels of Cyclins D1 and D3 in WT and *TIPE2*$^{-/-}$ VSMCs stimulated with PD98059 (a specific inhibitor of ERK1/2, 20 μM) plus Stattic (a specific compound that inhibits the activation and nucleus translocation of STAT3, 10 μM) following PDGF-BB treatment were analyzed by real-time PCR. $^{***}P < 0.001$, $^{**}P < 0.005$, n = 3.

subsequent proliferation of VSMCs by inactivating Rac1. Based on these results, we conclude that TIPE2 limits neointimal formation after vascular injury by regulating the proliferation of VSMCs; therefore, TIPE2 may be a new therapeutic target for the prevention of restenosis.

Coronary artery disease is the leading cause of mortality and morbidity in the developed world [30]. To date, percutaneous coronary intervention especially coronary stent placement is the preferred therapeutic method for coronary artery diseases [26,31–33]. However, several major clinical drawbacks still persist, including restenosis within the treated vessel [30,34]. Therefore, it is important to dissect the molecular mechanisms of restenosis to improve the safety and efficacy of PCI. Restenosis is mainly due to neointima formation and constrictive remodeling of blood vessel, which is caused primarily by the effects of VSMC proliferation and migration [35]. Growth factors such as PDGF and FGF released during the arterial injury caused by PCI play a central role in the pathogenesis of restenosis and mediate many important cellular processes including VSMC proliferation [1]. However, the molecular mechanisms controlling growth factor-induced VSMC proliferation and subsequent neointimal hyperplasia remain to be elucidated. PDGF is an important growth factor released after PCI and vascular injury and is related to VSMC proliferation and ensuing restenosis. Therefore, screening of molecules with potential to limit inappropriate proliferation of VSMCs in a PDGF shedding condition may be beneficial. We previously reported that TIPE2 acts as an atheroprotective molecule by inhibiting ox-LDL-induced dedifferentiation, migration and proliferation of VSMCs [14]. In this study we found for the first time that TIPE2 inhibited PDGF-BB-

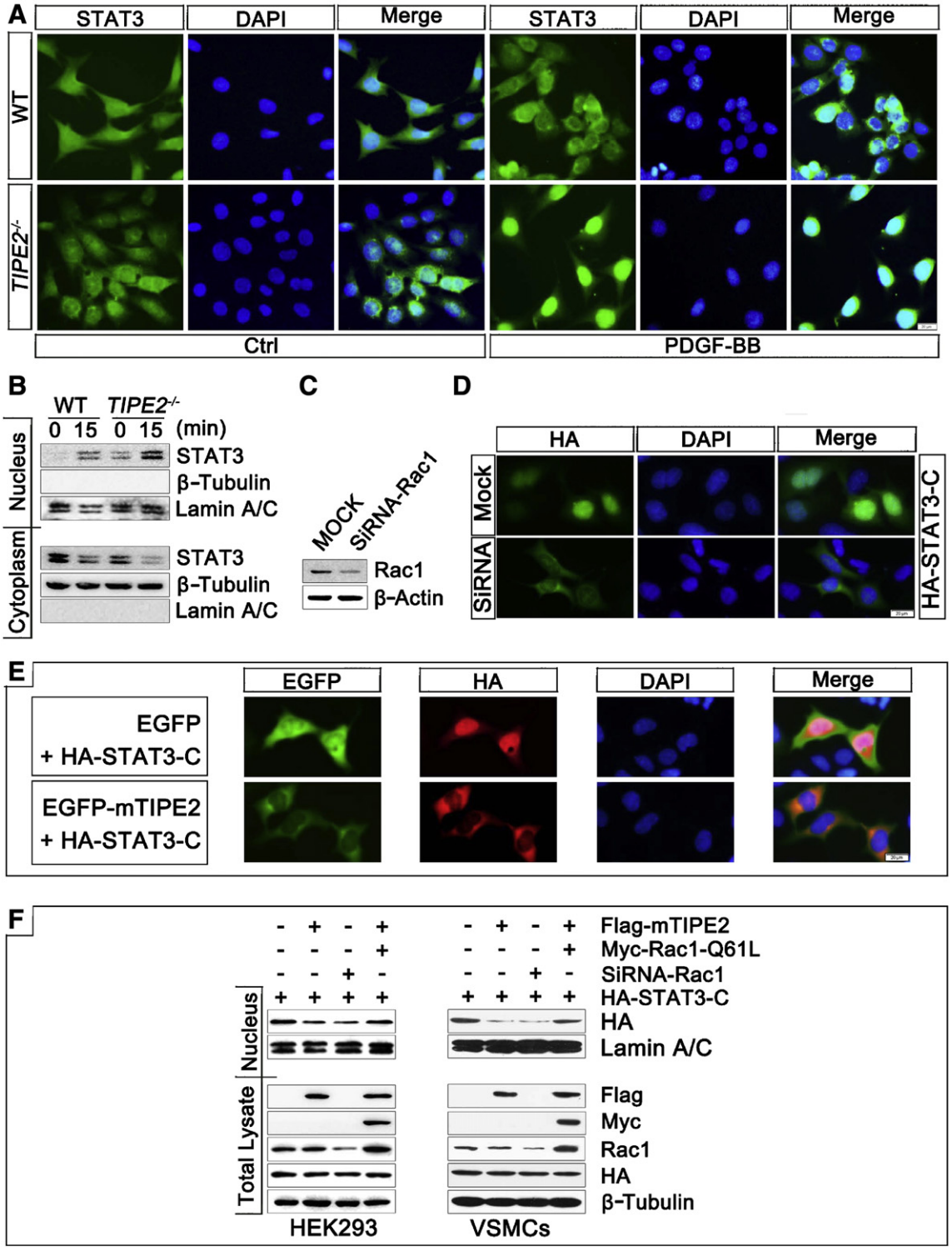

Fig. 6. TIPE2 modulates STAT3 nuclear translocation in a Rac1 dependent manner. (A) Nuclear transport of STAT3 in WT and *TIPE2*$^{-/-}$ VSMCs treated with PDGF-BB was evaluated by immunofluorescence staining. Scale bars indicate 20 μm. (B) PDGF-BB-induced redistribution of STAT3 in WT and *TIPE2*$^{-/-}$ VSMCs were examined by immunoblotting. β-Tubulin and Lamine A/C served as loading controls for cytoplasm and nucleus proteins, respectively. Three independent experiments were performed and one representative was shown. (C) Rac1 protein expression in HEK293 transfected with siRNA-Rac1 or siRNA-control (MOCK) was determined by immunoblotting. (D) Subcellular localization of HA-STAT3-C in HEK293 cells after addition of siRNA-Rac1 or MOCK was examined by immunofluorescence staining. Scale bars indicate 20 μm. (E) Subcellular localization of HA-STAT3-C in HEK293 cells after addition of EGFP-mTIPE2 or EGFP. Scale bars indicate 20 μm. (F) Subcellular distribution of HA-STAT3-C in HEK293 cells (left panel) and WT VSMCs (right panel) transfected with Flag-mTIPE2 plus Myc-Rac1-Q61L, Flag-mTIPE2 only, or siRNA-Rac1 was detected by immunoblotting. β-Tubulin and Lamine A/C served as loading controls for total and nucleus protein, respectively. Three independent experiments were performed and one representative was shown.

stimulated proliferation of VSMCs via inactivation of Rac1 and downstream signaling to ERK1/2 and STAT3. Regulation of the expression level of cell cycle regulatory molecules (including Cyclins, Cdks, Cdk inhibitors) is one of the principal mechanisms for inhibiting cell growth. Previous studies have reported that ERK1/2 and STAT3 modulated Cyclin D1 and D3 transcription and ensuing proliferation of VSMCs [26,27].

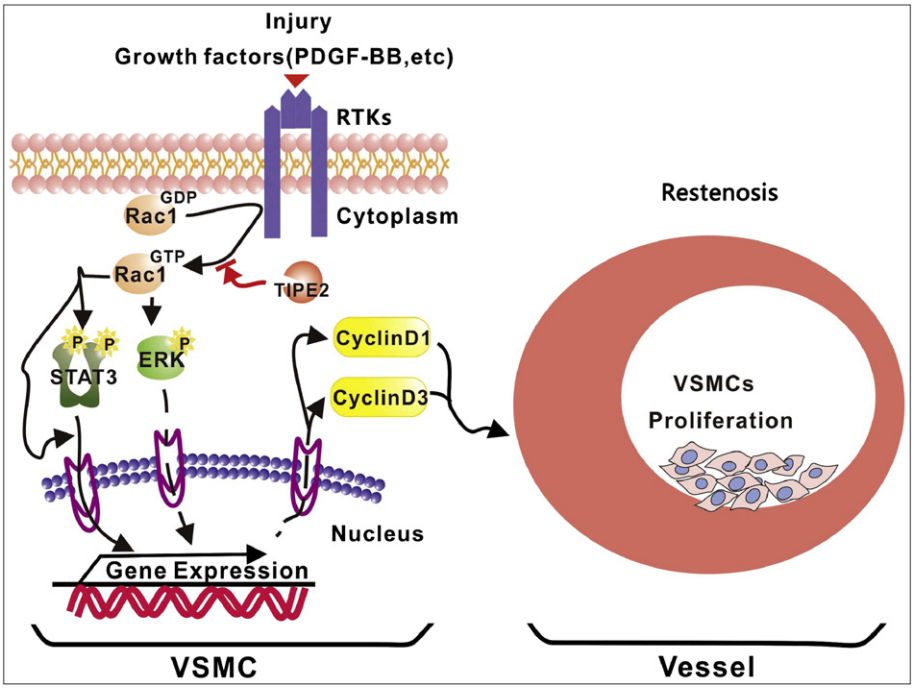

Fig. 7. Proposed roles of TIPE2 in vascular remodeling. In response to injury and growth factors such as PDGF-BB, Rac1 was activated in VSMCs. Activated Rac1 not only promoted the phosphorylation of both STAT3 and ERK1/2 but also advanced nucleus translocation of activated STAT3. STAT3 collaborated with ERK1/2 signaling to upregulate the expression of Cyclin D1 and Cyclin D3, both of which were required for the G_1/S phase transition and cell growth. TIPE2 acted as a negative regulator of the aforementioned processes by inhibiting Rac1 activation, herein limited the proliferation of VSMCs and the ensuing restenosis formation.

Consistent with this, here we showed that TIPE2 downregulates both Cyclin D1 and Cyclin D3 genes through ERK and STAT3 dependent mechanisms.

TIPE2 was first identified as a negative regulator of both inflammation and ras-related neoplasia [8–10]. TIPE2-dependent mechanism for anti-inflammation and anti-tumorgenesis has been well elucidated. However, less is known about TIPE2 in the modulation of cellular processes in non-immune organs. Our previous report provided initial evidence that TIPE2 inhibited ox-LDL-induced dedifferentiation of VSMCs in a manner dependent on ERK1/2 and P38 signal pathway. However, the upstream molecular mechanism by which TIPE2 modulated MAPK signaling is not completely clear. In our present study, we further demonstrated that TIPE2 affects PDGF-stimulated activation of ERK1/2 and STAT3, and ensuing nucleus translocation of STAT3 in VSMCs by interfering with Rac1. Rac is a member of the Rho family of small GTPases, which acts as a molecular switch to control a wide array of cellular functions [20]. Rac GTPase pathways is involved in various pathological conditions in humans, including tumorigenesis and some immune related diseases [36]. Therefore, TIPE2, as a novel inhibitory molecule of Rac, likely plays crucial roles in the aforementioned Rac-related diseases.

In conclusion, our data indicate that TIPE2 expressed in VSMCs plays a vascular protective role during the pathological process of injury-induced restenosis by negatively regulating PDGF-stimulated cellular proliferation (Fig. 7). These findings may not only advance our understanding of the molecular mechanisms controlling VSMC proliferation and subsequent neointimal hyperplasia, but also lead to the development of TIPE2-based strategies for treating restenosis.

Abbreviations

TIPE2	tumor necrosis factor (TNF) α-induced protein 8-like 2 (TNFAIP8L2)
SMαA	α-smooth muscle actin
VSMCs	vascular smooth muscle cells
WT	wild-type
mTIPE2	murine TIPE2
TIPE2$^{-/-}$	TIPE2 deficient
EDU	thymidine analog 5-ethynyl-2′-deoxyuridine
DAPI	4′,6-diamino-2-phenylindole

Transparency document

The Transparency document associated with this article can be found in the online version.

Funding

This work was supported by the grants from the National Natural Science Foundation of China (No. 81171578, No. 81100205), the key grant from the Health Department of Shandong Province (2009HD009), and the Award Funds for Excellent Young and Middle-aged Scientists of Shandong Province (BS2009YY007).

Conflict of interest

The authors have no conflict of interest to declare.

Acknowledgements

None.

References

[1] Z. Tang, Y. Wang, Y. Fan, Y. Zhu, S. Chien, N. Wang, Suppression of c-Cbl tyrosine phosphorylation inhibits neointimal formation in balloon-injured rat arteries, Circulation 118 (2008) 764–772.
[2] J. Kim, L. Zhang, K. Peppel, J.H. Wu, D.A. Zidar, L. Brian, S.M. DeWire, S.T. Exum, R.J. Lefkowitz, N.J. Freedman, Beta-arrestins regulate atherosclerosis and neointimal hyperplasia by controlling smooth muscle cell proliferation and migration, Circ. Res. 103 (2008) 70–79.
[3] I.D. Moussa, A. Colombo, Antiplatelet therapy discontinuation following drug-eluting stent placement: dangers, reasons, and management recommendations, Cathet. Cardiovasc. Interv.: Off. J. Soc. Card. Angiography Interv. 74 (2009) 1047–1054.

[4] A.A. Bavry, D.L. Bhatt, Appropriate use of drug-eluting stents: balancing the reduction in restenosis with the concern of late thrombosis, Lancet 371 (2008) 2134–2143.
[5] R. Wessely, New drug-eluting stent concepts, Nat. Rev. Cardiol. 7 (2010) 194–203.
[6] M. Ikesue, Y. Matsui, D. Ohta, K. Danzaki, K. Ito, M. Kanayama, D. Kurotaki, J. Morimoto, T. Kojima, H. Tsutsui, T. Uede, Syndecan-4 deficiency limits neointimal formation after vascular injury by regulating vascular smooth muscle cell proliferation and vascular progenitor cell mobilization, Arterioscler. Thromb. Vasc. Biol. 31 (2011) 1066–1074.
[7] X. Cao, L. Zhang, Y. Shi, Y. Sun, S. Dai, C. Guo, F. Zhu, Q. Wang, J. Wang, X. Wang, Y.H. Chen, Human tumor necrosis factor (TNF)-alpha-induced protein 8-like 2 suppresses hepatocellular carcinoma metastasis through inhibiting Rac1, Mol. Cancer 12 (2013) 149.
[8] H. Sun, S. Gong, R.J. Carmody, A. Hilliard, L. Li, J. Sun, L. Kong, L. Xu, B. Hilliard, S. Hu, H. Shen, X. Yang, Y.H. Chen, TIPE2, a negative regulator of innate and adaptive immunity that maintains immune homeostasis, Cell 133 (2008) 415–426.
[9] Z. Wang, S. Fayngerts, P. Wang, H. Sun, D.S. Johnson, Q. Ruan, W. Guo, Y.H. Chen, TIPE2 protein serves as a negative regulator of phagocytosis and oxidative burst during infection, Proc. Natl. Acad. Sci. U. S. A. 109 (2012) 15413–15418.
[10] Y. Gus-Brautbar, D. Johnson, L. Zhang, H. Sun, P. Wang, S. Zhang, L. Zhang, Y.H. Chen, The anti-inflammatory TIPE2 is an inhibitor of the oncogenic Ras, Mol. Cell 45 (2012) 610–618.
[11] Y. Zhang, X. Wei, L. Liu, S. Liu, Z. Wang, B. Zhang, B. Fan, F. Yang, S. Huang, F. Jiang, Y.H. Chen, F. Yi, TIPE2, a novel regulator of immunity, protects against experimental stroke, J. Biol. Chem. 287 (2012) 32546–32555.
[12] W. Xi, Y. Hu, Y. Liu, J. Zhang, L. Wang, Y. Lou, Z. Qu, J. Cui, G. Zhang, X. Liang, C. Ma, C. Gao, Y. Chen, S. Liu, Roles of TIPE2 in hepatitis B virus-induced hepatic inflammation in humans and mice, Mol. Immunol. 48 (2011) 1203–1208.
[13] Y. Lou, S. Liu, C. Zhang, G. Zhang, J. Li, M. Ni, G. An, M. Dong, X. Liu, F. Zhu, W. Zhang, F. Gao, Y.H. Chen, Y. Zhang, Enhanced atherosclerosis in TIPE2-deficient mice is associated with increased macrophage responses to oxidized low-density lipoprotein, J. Immunol. 191 (2013) 4849–4857.
[14] G. Zhang, W. Zhang, Y. Lou, W. Xi, J. Cui, M. Geng, F. Zhu, Y.H. Chen, S. Liu, TIPE2 deficiency accelerates neointima formation by downregulating smooth muscle cell differentiation, Cell Cycle 12 (2013) 501–510.
[15] A. Kumar, V. Lindner, Remodeling with neointima formation in the mouse carotid artery after cessation of blood flow, Arterioscler. Thromb. Vasc. Biol. 17 (1997) 2238–2244.
[16] T. Yoshida, K.H. Kaestner, G.K. Owens, Conditional deletion of Kruppel-like factor 4 delays downregulation of smooth muscle cell differentiation markers but accelerates neointimal formation following vascular injury, Circ. Res. 102 (2008) 1548–1557.
[17] X. Zhang, Y. Sun, R. Pireddu, H. Yang, M.K. Urlam, H.R. Lawrence, W.C. Guida, N.J. Lawrence, S.M. Sebti, A novel inhibitor of STAT3 homodimerization selectively suppresses STAT3 activity and malignant transformation, Cancer Res. 73 (2013) 1922–1933.
[18] G. Zhang, C. Hao, Y. Lou, W. Xi, X. Wang, Y. Wang, Z. Qu, C. Guo, Y. Chen, Y. Zhang, S. Liu, Tissue-specific expression of TIPE2 provides insights into its function, Mol. Immunol. 47 (2010) 2435–2442.
[19] M. Sata, A. Saiura, A. Kunisato, A. Tojo, S. Okada, T. Tokuhisa, H. Hirai, M. Makuuchi, Y. Hirata, R. Nagai, Hematopoietic stem cells differentiate into vascular cells that participate in the pathogenesis of atherosclerosis, Nat. Med. 8 (2002) 403–409.
[20] N.A. Mack, H.J. Whalley, S. Castillo-Lluva, A. Malliri, The diverse roles of Rac signaling in tumorigenesis, Cell Cycle 10 (2011) 1571–1581.
[21] J.E. Darnell Jr., The JAK-STAT pathway: summary of initial studies and recent advances, Recent Prog. Horm. Res. 51 (1996) 391–403 (discussion 403–394).
[22] T. Kawashima, Y.C. Bao, Y. Nomura, Y. Moon, Y. Tonozuka, Y. Minoshima, T. Hatori, A. Tsuchiya, M. Kiyono, T. Nosaka, H. Nakajima, D.A. Williams, T. Kitamura, Rac1 and a GTPase-activating protein, MgcRacGAP, are required for nuclear translocation of STAT transcription factors, J. Cell Biol. 175 (2006) 937–946.
[23] J.F. Bromberg, M.H. Wrzeszczynska, G. Devgan, Y. Zhao, R.G. Pestell, C. Albanese, J.E. Darnell Jr., Stat3 as an oncogene, Cell 98 (1999) 295–303.
[24] D.E. Levy, G. Inghirami, STAT3: a multifaceted oncogene, Proc. Natl. Acad. Sci. U. S. A. 103 (2006) 10151–10152.
[25] V.J. Dzau, R.C. Braun-Dullaeus, D.G. Sedding, Vascular proliferation and atherosclerosis: new perspectives and therapeutic strategies, Nat. Med. 8 (2002) 1249–1256.
[26] D.G. Sedding, M. Trobs, F. Reich, G. Walker, L. Fink, W. Haberbosch, W. Rau, H. Tillmanns, K.T. Preissner, R.M. Bohle, A.C. Langheinrich, 3-Deazaadenosine prevents smooth muscle cell proliferation and neointima formation by interfering with Ras signaling, Circ. Res. 104 (2009) 1192–1200.
[27] M.C. Simeone-Penney, M. Severgnini, L. Rozo, S. Takahashi, B.H. Cochran, A.R. Simon, PDGF-induced human airway smooth muscle cell proliferation requires STAT3 and the small GTPase Rac1, Am. J. Physiol. Lung Cell. Mol. Physiol. 294 (2008) L698–L704.
[28] Z. Li, J. Shen, W.K. Wu, X. Yu, J. Liang, G. Qiu, J. Liu, Leptin induces cyclin D1 expression and proliferation of human nucleus pulposus cells via JAK/STAT, PI3K/Akt and MEK/ERK pathways, PLoS One 7 (2012) e53176.
[29] I.T. Lee, C.C. Lin, C.H. Wang, W.J. Cherng, J.S. Wang, C.M. Yang, ATP stimulates PGE(2)/cyclin D1-dependent VSMCs proliferation via STAT3 activation: role of PKCs-dependent NADPH oxidase/ROS generation, Biochem. Pharmacol. 85 (2013) 954–964.
[30] A. Curcio, D. Torella, C. Indolfi, Mechanisms of smooth muscle cell proliferation and endothelial regeneration after vascular injury and stenting: approach to therapy, Circ. J.: Off. J. Jpn. Circ. Soc. 75 (2011) 1287–1296.
[31] C. Indolfi, M. Pavia, I.F. Angelillo, Drug-eluting stents versus bare metal stents in percutaneous coronary interventions (a meta-analysis), Am. J. Cardiol. 95 (2005) 1146–1152.
[32] E.L. Wallace, A. Abdel-Latif, R. Charnigo, D.J. Moliterno, B. Brodie, R. Matnani, K.M. Ziada, Meta-analysis of long-term outcomes for drug-eluting stents versus bare-metal stents in primary percutaneous coronary interventions for ST-segment elevation myocardial infarction, Am. J. Cardiol. 109 (2012) 932–940.
[33] J.A. Bittl, Y. He, A.K. Jacobs, C.W. Yancy, S.L. Normand, G. American College of Cardiology Foundation/American Heart Association Task Force on Practice, Bayesian methods affirm the use of percutaneous coronary intervention to improve survival in patients with unprotected left main coronary artery disease, Circulation 127 (2013) 2177–2185.
[34] W.A. Gray, J.F. Granada, Drug-coated balloons for the prevention of vascular restenosis, Circulation 121 (2010) 2672–2680.
[35] A. Farb, D.K. Weber, F.D. Kolodgie, A.P. Burke, R. Virmani, Morphological predictors of restenosis after coronary stenting in humans, Circulation 105 (2002) 2974–2980.
[36] S.Y. Pai, C. Kim, D.A. Williams, Rac GTPases in human diseases, Dis. Markers 29 (2010) 177–187.